

# PCCP

Accepted Manuscript



This is an *Accepted Manuscript*, which has been through the Royal Society of Chemistry peer review process and has been accepted for publication.

*Accepted Manuscripts* are published online shortly after acceptance, before technical editing, formatting and proof reading. Using this free service, authors can make their results available to the community, in citable form, before we publish the edited article. We will replace this *Accepted Manuscript* with the edited and formatted *Advance Article* as soon as it is available.

You can find more information about *Accepted Manuscripts* in the [Information for Authors](#).

Please note that technical editing may introduce minor changes to the text and/or graphics, which may alter content. The journal's standard [Terms & Conditions](#) and the [Ethical guidelines](#) still apply. In no event shall the Royal Society of Chemistry be held responsible for any errors or omissions in this *Accepted Manuscript* or any consequences arising from the use of any information it contains.

## Singlet lifetime measurements in an all-proton chemically equivalent spin system by hyperpolarization and weak spin lock transfers

Received 00th January 20xx,  
Accepted 00th January 20xx

DOI: 10.1039/x0xx00000x

Y. Zhang, K. Basu, J. W. Canary and A. Jerschow\*

www.rsc.org/

Hyperpolarized singlet states provide the opportunity for polarization storage over periods significantly longer than  $T_1$ . Here, we show how that the singlet state in a chemically equivalent proton spin system can be revealed by a weak power spin-lock. This procedure allowed the measurement of the lifetimes of the singlet state in protic solvents. The contributions of different intra- and intermolecular relaxation mechanisms to singlet lifetimes are investigated with this procedure.

### Introduction

Hyperpolarization and singlet state NMR can be combined to form powerful methodology for overcoming the limitations of low sensitivity and short lifetimes. Molecules, hyperpolarized by para-hydrogen induced polarization (PHIP)<sup>1-3</sup> can be sources of such long-lived singlet order. Several methods exist for revealing this silent singlet state, including field cycling,<sup>4</sup> pulse sequences<sup>5-10</sup> and chemical reactions.<sup>11, 12</sup> Recently, the Spin Lock Induced Crossing (SLIC) method was successfully used in a chemically inequivalent 2-spin system<sup>10</sup> and a heteronuclear chemically equivalent 4-spin system.<sup>8, 13</sup>

Here, we show that the PHIP-originated singlet state in a homonuclear 4-spin system can be revealed by a weak-power SLIC, despite the very low degree of inequivalence, and the long transfer times needed. In the molecule investigated here, the inequivalence originates from an out-of-pair coupling constant difference of about 0.4 Hz. The small degree of inequivalence required the use of hyperpolarization, since a sequence based on triplet-to-singlet and singlet-to-triplet conversions on thermal samples was not sensitive enough.

In the approach used here, a multi-conversion method readout sequence<sup>9</sup> is used to measure the lifetimes in water-diluted solvents in order to study the influence of intermolecular coupling from solvent protons. Furthermore, the influence of dissolved oxygen on singlet state life times is investigated as well. Besides the residual intramolecular dipolar couplings, chemical shift anisotropy (CSA), in particular

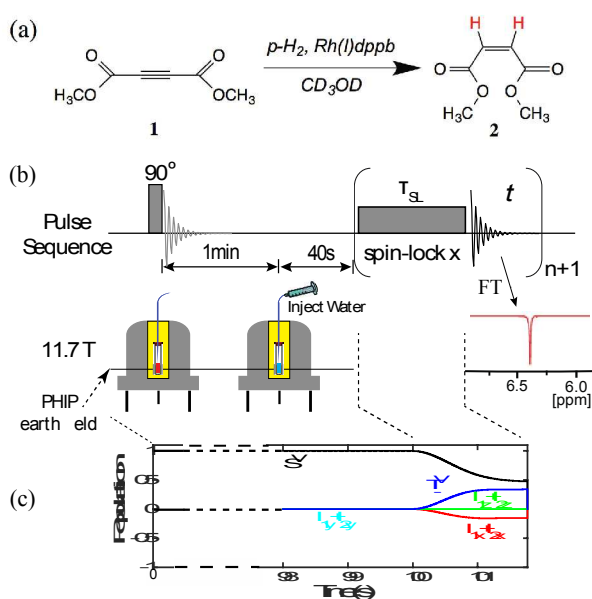


**Fig. 1** (a) Reaction scheme. Dimethyl acetylene dicarboxylate (DMAD; **1**) was hydrogenated at earth magnetic field with *para*-hydrogen to yield hyperpolarized dimethyl maleate (DMM; **2**) in methanol. (b) Pulse sequence and water dilution experienced by the sample. The observed signal is shown in red. (c) Simulation of SLIC experiment after PHIP.  $S^V$  and  $T^V$  and the spin operator terms label the curves of the polarizations of the singlet and triplet states of the vinylene protons in **2**.

the antisymmetric component thereof, is found to contribute significantly to the singlet lifetime shortening in these  $^1\text{H}$  NMR studies, in line with previous work on  $^{13}\text{C}$  singlets.<sup>14</sup> These studies were performed in protic solvent mixtures, and may thus provide upper limits on proton singlet state life times that can be expected in aqueous solutions. The use of weak power singlet-to-triplet conversion has advantages over the strong

Department of Chemistry, New York University  
100 Washington Sq. East, New York, NY 10003 USA

\* E-mail: alexej.jerschow@nyu.edu

Homepage: <http://www.nyu.edu/projects/jerschow/>

Electronic Supplementary Information (ESI) available: [details of any supplementary information available should be included here]. See DOI: 10.1039/x0xx00000x

power conversion methods in terms of lower power deposition and being selective for a particular group of spins.

## Methods

Dimethyl acetylene dicarboxylate (DMAD; **1**) was hydrogenated in methanol at earth magnetic field with para-hydrogen to yield hyperpolarized dimethyl maleate (DMM; **2**) (Fig 1a), a symmetric homonuclear 4-spin system that has a long-lived nuclear singlet state.<sup>4, 11</sup> The NMR sample tube, loaded with a syringe containing water, was inserted into the NMR magnet operating at a field of 11.7 T. Subsequently, a 90° pulse was used to spoil the signal resulting from the transport across different magnetic fields. After 1 min, when the hydrogenation reaction completed (ESI Fig. 1), a specified amount of water was injected into the NMR tube to give the desired water/methanol solvent mixture. After another delay of 40 s to allow for adequate solvent mixing (ESI Fig. 2), the singlet state was revealed by a multi-conversion SLIC sequence (Fig. 1b). For the samples without further water dilution, the pulses were executed immediately after 1 min.

The simulation of singlet population changes in PHIP and SLIC experiments is shown in Fig. 1c. Immediately after PHIP preparation, the singlet state of the vinylenes protons,  $S^v$ , is generated in **2**. After SLIC, singlet population was converted to observable transverse triplet-state population. SLIC was performed using a continuous-wave spin lock on resonance with the vinylenes protons in DMM. The nutation frequency was found to be optimal at 11.6 Hz, which should equal the  $J$  coupling between the vinylenes protons (see Theory section). The spin-lock duration,  $\tau_{SL}$ , was optimized to 1.77s (ESI Fig. 3), which indicates that the out-of-pair  $J$  coupling difference was about 0.4 Hz, lower than previously thought.<sup>4, 9</sup>

CSA tensors and  $J$ -couplings were calculated using Gaussian09.<sup>15</sup> Geometry optimization was performed with a b3lyp/6-311+g(d,p) functional/basis set combination and the Cs symmetry constraint, and the tensors and coupling constants were obtained from a GIAO calculation with the 'spinspin' and 'mixed' keywords and a b3lyp/aug-cc-pVTZ combination. This calculation gave the couplings between the vinylenes protons as 8.3 Hz and the out of pair couplings as -0.13 Hz and -0.05 Hz.

Symbolic calculations and relaxation expressions were performed by MathNMR and verified by hand.<sup>16</sup> The package

**TABLE 1** Degassing preparation protocol and composition of the final solvent for each sample (after water injection). Samples with degassing by bubbling are coded as B1 - B5. Freeze-Pump-Thaw (FPT) samples are coded as F1, F3, and F5. "N/A" indicates no water injected.

Sample	Final Solvent	MeOD	H <sub>2</sub> O or D <sub>2</sub> O
B1	100% MeOD	No degass	N/A
B2	D <sub>2</sub> O : MeOD = 0.5:1	No degass	Bubbled
B3	D <sub>2</sub> O : MeOD = 1:1	No degass	Bubbled
B4	H <sub>2</sub> O : MeOD = 0.5:1	No degass	Bubbled
B5	H <sub>2</sub> O : MeOD = 1:1	No degass	Bubbled
F1	100% MeOD	FPT	N/A
F3	D <sub>2</sub> O : MeOD = 1:1	FPT	FPT
F5	H <sub>2</sub> O : MeOD = 1:1	FPT	FPT

has been recently updated to include antisymmetric CSA relaxation calculations.<sup>17</sup> Numerical calculations were performed with MATLAB.

Experiments were performed with oxygen removal by two different methods: (1) Bubbling nitrogen gas through the water solution (H<sub>2</sub>O and D<sub>2</sub>O) for 30 min prior to injection; methanol solutions were not degassed in these samples, but were used as received (sealed vials). Five samples were prepared, with different amounts of water dilution. The terminal water/methanol volume ratio of each sample is shown in Table 1. They are coded as B1, B2, B3, B4, and B5. (2) The freeze-pump-thaw (FPT) technique was used to degas both the methanol solution and water solution for injection. The samples were placed in Schlenck tubes, frozen in liquid nitrogen, and thawed to release dissolved gasses. The cycle was repeated for both methanol and water at least for four cycles. Three samples using the two procedures are coded as F1, F3 and F5.

The resonance frequency of the vinylenes protons of DMM in the final solution changed slightly over the course of 40 s, likely as a result of a changing lock field after dilution. About 30Hz of vinylenes proton frequency change was seen immediately after injection of water and another 1.3Hz-shift before the end of the waiting period. The frequency of the conversion pulse had to be adjusted accordingly, in order to insure an efficient conversion.

## Theory

The proton-only AA'X<sub>3</sub>X'<sub>3</sub> spin-system of DMM was previously treated as a AA'XX' system for ease of describing overall singlet-to-triplet transitions.<sup>4</sup> In order to investigate the influence of the multiplicity on singlet-to-triplet transitions, symmetry-adapted bases were also introduced for AA'X<sub>n</sub>X'<sub>n</sub> systems.<sup>13</sup> These bases may not always provide a useful interpretation, however. For example, in the DMM molecule, it is highly unlikely that singlet states between the methyl groups will ever be created. Furthermore, their lifetimes would not be expected to be particularly long, because relaxation processes would be largely uncorrelated between those groups. We therefore provide here a description, which avoids complications arising from a symmetry-adapted basis, but also allows one to include the effects of the methyl multiplicity.

The vinylenes protons are weakly coupled to the methyl protons, and it is legitimate to assume that the coupling between the methyl groups is negligible. In the following discussion we use the symbols  $J_V$  for the vinylenes-vinylenes coupling constant and  $J_{VM1}$  and  $J_{VM2}$  for the two out-of-pair coupling constants. The superscripts V1, V2, M1, M2 are used to label the spin operators for the two vinylenes and methyl groups, respectively. The Hamiltonian of the system is given by

$$\frac{H}{\hbar} = \nu_V(I_z^{V1} + I_z^{V2}) + J_V I^{V1} \cdot I^{V2} + \sum_{i=1}^3 [ \nu_M (I_{iz}^{M1} + I_{iz}^{M2}) + J_{VM1} (I_z^{V1} I_{iz}^{M1} + I_z^{V2} I_{iz}^{M2}) + J_{VM2} (I_z^{V1} I_{iz}^{M2} + I_z^{V2} I_{iz}^{M1}) ] \quad (1)$$

where we have used the weak coupling approximation for the vinylene-methyl couplings. We now consider the situation during a weak rf field with nutation frequency  $\nu_1$  applied selectively on-resonance with the vinylene signals. We can then use a frame rotating at  $\nu_V$  for the vinylene, and at  $\nu_M$  for the methyl operators, which gives

$$\nu_1(I_x^{V1} + I_x^{V2}) + J_V I^{V1} \cdot I^{V2} + \sum_{i=1}^3 [J_{VM1}(I_z^{V1} I_{iz}^{M1} + I_z^{V2} I_{iz}^{M2}) + J_{VM2}(I_z^{V1} I_{iz}^{M2} + I_z^{V2} I_{iz}^{M1})] \quad (2)$$

Writing the Hamiltonian in a frame that diagonalizes the  $I_x^{V1,2}$  operators, one obtains for the vinylene subspace the form

$$\frac{\tilde{H}}{\hbar} = \begin{bmatrix} \nu_1 + \frac{J_V}{4} & A & B & 0 \\ A & -\frac{J_V}{4} & \frac{J_V}{2} & B \\ B & \frac{J_V}{2} & -\frac{J_V}{4} & A \\ 0 & B & A & \frac{J_V}{4} - \nu_1 \end{bmatrix} \quad (3)$$

where  $A = -\frac{J_{VM1}m_{M2} + J_{VM2}m_{M1}}{2}$ , and  $B = -\frac{J_{VM1}m_{M1} + J_{VM2}m_{M2}}{2}$ , and  $m_{M1,2}$  are the magnetic quantum numbers of the methyl spins. Finally, a transformation into the singlet-triplet basis

$$\{T_1, T_0, T_{-1}, S_0\} = \{|\uparrow\uparrow\rangle, 1/\sqrt{2}(|\uparrow\downarrow\rangle + |\downarrow\uparrow\rangle), |\downarrow\downarrow\rangle, 1/\sqrt{2}(|\uparrow\downarrow\rangle - |\downarrow\uparrow\rangle)\} \quad (4)$$

of that frame gives:

$$\frac{\tilde{H}_{T,S}}{\hbar} = \begin{bmatrix} \nu_1 + \frac{J_V}{4} & C & 0 & -D \\ C & \frac{J_V}{4} & C & 0 \\ 0 & C & \frac{J_V}{4} - \nu_1 & D \\ -D & 0 & D & -\frac{3J_V}{4} \end{bmatrix} \quad (5)$$

where  $C = -\frac{(J_{VM1} + J_{VM2})(m_{M1} + m_{M2})}{2\sqrt{2}}$ ,  $D = \frac{(J_{VM1} - J_{VM2})(m_{M1} - m_{M2})}{2\sqrt{2}}$ .

Eq. (5) reveals that by choosing  $\nu_1 = J_V$  one can bring the states  $T_{-1}$ , and  $S_0$  into resonance with each other. At this point, the matrix element  $D$  causes interconversion between the two. It can be seen that choosing a time for the spin lock according to

$$\tau_{SL} = \frac{1}{(J_{VM1} - J_{VM2})(m_{M1} - m_{M2})} \quad (6)$$

maximizes the conversion frequency. The conversion rates thus vary by factors of up to three. A numerical simulation using the 4x4 subspace of Eq. (5) shows that the maximum transfer to  $T_{-1}$  is obtained at

$$\tau_{SL} = \frac{\sqrt{2}}{2(J_{VM1} - J_{VM2})} \quad (7)$$

which is in line with previous treatments.<sup>8,13</sup>

### Multiple conversion

A single conversion by SLIC produces a relatively weak signal due to the small degree of inequivalence in DMM and some

relaxation and inhomogeneity losses during the transfer. Franzoni et al.<sup>9</sup> have demonstrated a multiple-conversion approach for the strong power conversion method, by which one can perform several measurements following a single polarization step. By this procedure, repeated conversion and readouts followed by acquisition and a waiting time  $\Delta t$  as indicated in Fig. 1, can be used to derive both the conversion efficiency and the singlet state lifetime. This approach is also applicable for the low power conversion. The signal detected after the  $n$ -th conversion step is

$$F_n = F_0(1 - \xi)^n \exp\left(-\frac{n\Delta t}{T_S}\right), \quad (8)$$

where  $F_0$  is the signal observed in the first readout,  $T_S$  is the singlet state life time, and  $\xi$  is the fraction of the singlet order lost during the conversion step. Fitting  $F_n/F_0$  to an exponential decay as a function of  $n$  provides a decay rate of

$$\lambda = \frac{1}{T_S} \Delta t - \ln(1 - \xi). \quad (9)$$

When plotted over several experiments with different  $\Delta t$ , this procedure provides both  $T_S$  and  $\xi$ .<sup>9</sup> One advantage of this approach is that one can measure both parameters independently of the initial average polarization level.<sup>9</sup> This property is particularly advantageous for cases where different parts of the sample complete their reactions or the mixing processes at different times. Although originally called the 'conversion efficiency',<sup>9</sup> the factor  $\xi$  actually measures the polarization lost from the singlet-state during one conversion step. Since not all polarization lost from the singlet state ends up being detectable, the actual conversion efficiency is often significantly lower. This effect is also clearly seen in the simulation in Fig. 1.

### Singlet-state relaxation mechanisms

The various mechanisms by which singlet states can relax have been described by Levitt, Pileio and coworkers.<sup>6,18-24</sup> In the absence of a spin lock, singlet-triplet leakage may be estimated by considering the  $T_1$  values measured for the vinylene groups, and the coupling constants.<sup>14,25</sup> The singlet and triplet states are separated by  $J_V$  in energy and the off-diagonal elements between them have a magnitude equal to  $D$ . From perturbation theory, the leakage decay rate can be derived as<sup>14,25</sup>

$$\frac{2\pi(J_{VM1} - J_{VM2})(m_{M1} - m_{M2})}{T_1 \left[ \left(\frac{1}{T_1}\right)^2 + (2\pi J_V)^2 \right]}, \quad (10)$$

which is significantly smaller than  $1/T_1$  when the out-of-pair coupling difference is much smaller than the intra-singlet coupling constant.

The intra-singlet dipolar coupling does not affect the singlet lifetime, but out-of-pair couplings do.<sup>8</sup> It has been reported that in the absence of these couplings, the major lifetime limiting mechanism for <sup>13</sup>C singlets is the chemical shift anisotropy (CSA) mechanism (and the antisymmetric CSA, in particular).<sup>26</sup> In that work the relaxation contributions of CSA have been calculated for the extreme narrowing limit. Without this restriction, the expressions for the relaxation rates due to CSA can be determined as

$$R_S^{g+} = \frac{2}{45} \omega_0^2 \|\Delta\sigma_+\|^2 \left[ 2\tau_2 + 3 \frac{\tau_2}{1 + (\omega_0\tau_2)^2} \right] \\ R_S^{g-} = \frac{2}{9} \omega_0^2 \|\Delta\sigma_-\|^2 \frac{\tau_1}{1 + (\omega_0\tau_1)^2} \quad (11)$$

where  $\omega_0$  is the Larmor frequency in angular frequency units,  $\Delta\sigma_{\pm}$  is the difference between the CSA tensors of the two

nuclei participating in the singlet, with the 'plus' index referring to the symmetric and trace-less portion of that tensor, and the 'minus' index to the antisymmetric portion, the norm  $\|\Delta\sigma_{\pm}\|$  indicates the square root of the sum of the squares of all the matrix elements in the respective tensor, and  $\tau_{1,2}$  are the first and second rank correlation times, respectively, with  $\tau_1 = 3\tau_2$ .

We consider further the contributions of intermolecular dipolar couplings (from solvent protons), and relaxation induced by interactions with paramagnetic oxygen. Although detailed molecular models can be developed,<sup>21</sup> these are not always practical, due to the number of parameters that may not be known to sufficient accuracy, such as, for example, the average molecular radii, and effects of proton hopping. We use here the treatment considered in Ref. <sup>24</sup>, where intermolecular relaxation is described via an external random field. This description allows one to characterize the degree of correlation between the effects of a relaxation mechanism on both spins that participate in a singlet state. Under the extreme narrowing condition, which applies here, the ratio between the  $T_5$  and  $T_1$  relaxation contributions due to these intermolecular relaxation mechanisms can be described by

$$K = \frac{R_S}{R_1} = 2 \frac{B_1^2 + B_2^2 - 2CB_1B_2}{B_1^2 + B_2^2}, \quad (12)$$

where  $B_{1,2}$  are the root mean square magnetic fields generated at the sites of either nuclear spin due to solvent protons or dissolved oxygen, and  $C$  is the correlation coefficient between the fields. The ratio  $K$  is equal to two in the case of no correlation, and tends to zero in the case of complete correlation ( $C = 1$ ).<sup>24</sup>

## Results and discussion

Typical spectra of the long-lived nuclear singlet state observed by multi-conversion SLIC can be found in ESI Fig. 4, and the all the raw data from the sequence are displayed there as well. The decay rate  $\lambda$  of the signal after repeated conversion as a function of the number of additional conversion blocks,  $n$ , is plotted in Fig. 2. A linear relationship is found according to Eq. (9).

The extracted lifetimes of the singlet state,  $T_S$ , and the

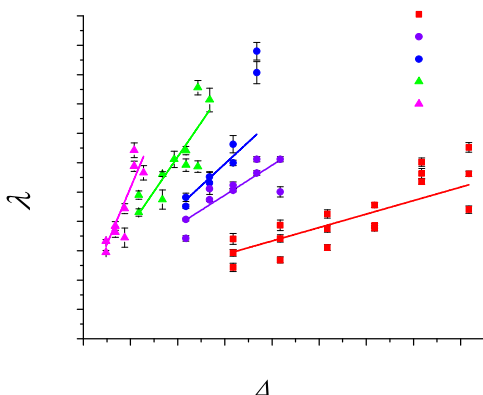


Fig. 2 Decay constant,  $\lambda$ , plotted as a function of time interval  $\Delta t$ . The legend shows corresponding samples as coded in Table 1.

measured  $T_1$  values of vinylene protons in different samples

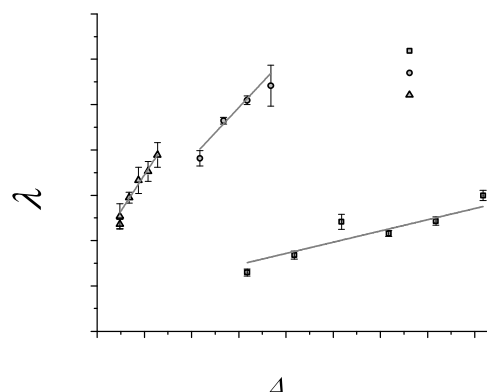


Fig. 3 Data for freeze-pump-thaw samples. The legend shows corresponding samples as coded in Table 1.

are summarized in Table 2. All the  $T_1$  values were measured with the same samples as the  $T_S$  values (in terms of bubbling vs. FPT preparation). The longest singlet lifetime observed was 353.4 s, with shorter times for higher proton concentrations, and higher oxygen concentration (B samples). As more water is added to the solution,  $T_S$  decreases. One reason for this decrease is the effect of increasing viscosity, and the other is the larger contribution of the intermolecular relaxation mechanisms as discussed below.

Given the shortest  $T_1$  constant found in our studies (6.4 s), and the coupling constants found experimentally, the singlet-triplet leakage rate can be calculated from Eq. (10) as  $2.22 \times 10^{-7} \text{ s}^{-1}$ , which would correspond to a life time of 75 min. An exact numerical calculation gives 83 min, also much longer than any reported singlet state life times for this molecule. This leakage mechanism can therefore be neglected in the ensuing discussion.

The norms of the differences in the symmetric and antisymmetric CSA tensors between the vinylene protons were determined from Gaussian09 calculations as  $\|\Delta\sigma_{+}\| = 5.71$  ppm, and  $\|\Delta\sigma_{-}\| = 3.87$  ppm, respectively. The rotational correlation times of the molecules can be determined from the viscosity of the solution by

$$\tau_r = \frac{4\pi\eta r^3}{3k_B T}. \quad (13)$$

TABLE 2 Summary of  $T_1$ , singlet lifetime ( $T_S$ ),  $1/K = T_S / T_1$ , and singlet conversion loss factor ( $\xi$ ).

Sample	$T_S$ (s)	$T_1$ (s)	$1/K$	$\xi$ (%)
B1	$218.4 \pm 11.4$	22.90	9.54	13.93
B2	$98.4 \pm 13.8$	12.07	8.15	16.81
B3	$67.2 \pm 3.6$	11.84	5.68	13.93
B4	$42.6 \pm 1.8$	6.41	6.65	13.93
B5	$27.0 \pm 4.2$	5.71	4.73	14.14
F1	$353.4 \pm 19.2$	23.90	14.79	13.93
F3	$78.0 \pm 1.2$	12.06	6.47	19.16
F5	$62.4 \pm 3.6$	6.40	9.75	22.86

**TABLE 3.** Differences in relaxation rates between samples B1 and F1 as coded in Table 1.  $i = 1, 3, 5$ .  $\Delta R_s(i) = 1/T_s(\text{Bi}) - 1/T_s(\text{Fi})$  ( $10^3\text{s}^{-1}$ ),  $\Delta R_1(i) = 1/T_1(\text{Bi}) - 1/T_1(\text{Fi})$  ( $10^3\text{s}^{-1}$ ).

$i$	1	3	5
$\Delta R_s(i)$	1.75	2.09	20.66
$\Delta R_1(i)$	1.83	1.54	18.88
$K(i) = \Delta R_s(i) / \Delta R_1(i)$	0.96	1.36	1.09

Given the reported viscosities,<sup>27, 28</sup> the average radius of the molecule as determined from the density and the molecular weight of DMM (3.68 Å), and assuming rigid molecular rotation, the correlation times are 27.6, 80.7, and 93.4 ps for samples B1(F1), B5(F5), and B3(F3), respectively. Using these numbers and the aforementioned CSA tensor norms, one obtains from Eq. (11) estimates for the contribution to the singlet state relaxation rates as  $1.97 \times 10^{-3}\text{s}^{-1}$ ,  $5.56 \times 10^{-3}\text{s}^{-1}$ ,  $6.36 \times 10^{-3}\text{s}^{-1}$  for the symmetric CSA mechanism, and  $2.55 \times 10^{-3}\text{s}^{-1}$ ,  $5.04 \times 10^{-3}$ ,  $5.19 \times 10^{-3}\text{s}^{-1}$  for the antisymmetric CSA mechanism for the corresponding motional regimes. The antisymmetric contribution is the stronger one in the extreme narrowing regime, and while both CSA rates become larger with increasing correlation times, the relative importance of the antisymmetric contribution decreases with increasing correlation times.

From the dipolar couplings derived from the geometry from the *ab initio* calculations, one can obtain the contributions of the vinylene-methyl dipolar couplings to the relaxation rates. This was done by first averaging over the methyl motion by calculating the averages of the inverse cube distances, before inserting these into the dipolar relaxation expressions. The intramolecular dipolar coupling relaxation rates are thus  $3.02 \times 10^{-3}\text{s}^{-1}$ ,  $9.40 \times 10^{-3}\text{s}^{-1}$ , and  $11.7 \times 10^{-3}\text{s}^{-1}$ , for the three selected correlation times, which shows that these are of approximately equal importance as the sum of the CSA contributions. These rates could be slightly higher if significant intra-molecule motion occurred, because cross-correlated contributions would be reduced.

It is noted that these calculated mechanisms would indicate a maximum singlet state lifetime that is significantly shorter than the measured life times (at least for sample F1). This indicates that CSA/dipole-dipole cross correlations may be at play to partly reduce the rates. It is also noted that the calculations assumed a molecule in vacuum and relied on reported viscosities, which may not fully reflect the experimental conditions.

In order to determine the effect of oxygen on the singlet state relaxation, experiments were performed with Freeze-Pump-Thaw (FPT) cycles (Fig. 3). Table 3 shows the differences of the relaxation rates between samples B1 and F1, B3 and F3, and B5 and F5. The data for samples B1-B5 are more scattered (Fig. 2) compared to those for F1, F3 and F5 (Fig. 3), likely as a result of larger variations in O<sub>2</sub> concentrations in the samples, and perhaps also larger uncertainties in singlet-triplet conversion efficiencies. Clearly, FPT is able to remove more oxygen. When taking the difference in the relaxation rates of samples with different oxygen concentrations, we obtain the relaxation contribution of oxygen. From the  $K$  ratio  $\Delta R_s/\Delta R_1$  we can then obtain an indication of the correlation coefficient  $C$  for the intermolecular relaxation mechanism according to Eq.

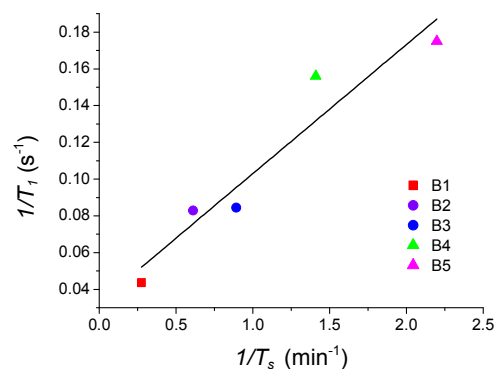


**Fig. 4** The correlation between  $T_s$  relaxivity ( $\text{s}^{-1}$ ) and  $T_1$  relaxivity ( $\text{s}^{-1}$ ) for samples B1-B5. B1 (red square), B2 (purple circle), B3 (blue circle), B4 (green triangle), B5 (pink triangle).

(12) for the different samples. In all cases, a sizable correlation of the paramagnetic mechanism is found, with the lowest one found for the B3(F3) solvent.

As seen in Figure 4,  $1/T_1$  and  $1/T_s$  are correlated when considering the B1-B5 and F1, F3, F5 (ESI Fig. 5) series separately. As expected, the slope is larger for samples F1, F3, F5, indicating that the degree of correlation between the relaxation mechanisms acting on the two spins in the singlet is smaller for oxygen-induced relaxation than it is for other mechanisms.

For sample F1, the experimental life time is much longer than the theoretically predicted life time based on intramolecular mechanisms along, which indicates that the oxygen removal procedure via FPT is very good. For samples B4 and B5, however, additional intermolecular relaxation contributions induced by solvent protons need to be considered.

The slopes of  $1/T_1$  and  $1/T_s$  as a function of proton concentration in the solution were determined as  $2.00 \times 10^3 \text{s}^{-1}\text{M}^{-1}$ , and  $4.56 \times 10^2 \text{s}^{-1}\text{M}^{-1}$  for samples B1-B5 and  $1.70 \times 10^3 \text{s}^{-1}\text{M}^{-1}$ , and  $1.48 \times 10^2 \text{s}^{-1}\text{M}^{-1}$  for samples F1, F3, F5, respectively. One can see that the relaxivities are overall lower in samples F1, F3 and F5, as expected, due the effect of residual oxygen in B1-B5. The  $K$ -value from this data is 0.087. This means that the correlation between the effects of intermolecular dipolar relaxation on both singlet protons is much larger than the one for the oxygen-induced relaxation mechanism. This finding is in line with the small difference in the  $T_s$  values between samples F3 and F5, while the differences in  $T_1$  values are much larger. In our analysis, we have neglected relaxation contributions from intra- and intermolecular relaxation mechanisms from deuterium, but these are likely much smaller than the mechanisms considered here.<sup>21</sup>

## Conclusions

The hyperpolarized singlet state stored in a chemically equivalent homonuclear 4-spin system was revealed by a weak

rf irradiation (SLIC), and showed a  $^1\text{H}$ - $^1\text{H}$  singlet lifetime of up to 5.9 minutes. A much longer duration of spin-lock is required for this homonuclear case than for the heteronuclear studies considered previously,<sup>8,13</sup> due to the tiny differences between the out-of-pair  $J$ -couplings. We find that the major contribution to singlet-state relaxation comes from intermolecular effects, with the strongest coming from paramagnetic oxygen, followed by a much weaker contribution from solvent protons. When excluding these factors, the major remaining relaxation contribution arises in approximately equal parts from the long-range intramolecular dipolar interactions, and the CSA mechanism. The antisymmetric CSA mechanism is the dominant contribution in the extreme narrowing limit, in line with recent  $^{13}\text{C}$  singlet studies.<sup>14, 29</sup> Outside of the extreme narrowing regime, the symmetric CSA contribution becomes dominant. In the absence of CSA contributions, such as would be the case in a molecule with inversion symmetry,<sup>23</sup> the only remaining life time limits would be due to singlet-triplet leakage, and as discussed recently, a spin-torsion mechanism.<sup>23</sup> It is also found that the correlation between the relaxation effects acting on the spins within the singlet are much larger for the intermolecular paramagnetic mechanism than for the intermolecular dipolar coupling mechanism. These studies point to the limitations of lifetimes that can be achievable for proton singlet states in protic solvents.

### Acknowledgements

This work was supported by NSF grants CHE-1412568 (J.C.), CHE-0957586 (A.J.) and the Margaret and Herman Sokol Doctoral Fellowship 2014-2015 (Y. Z.). The experiments were performed in the Shared Instrument Facility of the Department of Chemistry, New York University, supported by the US National Science Foundation under Grant No. CHE0116222. We thank P. C. Soon for help and discussions, and we acknowledge helpful discussions with Ranajeet Ghose about relaxation mechanisms.

### Notes and references

- 1 C. R. Bowers and D. P. Weitekamp, *Phys. Rev. Lett.*, 1986, **57**, 2645-2648.
- 2 C. R. Bowers and D. P. Weitekamp, *J. Am. Chem. Soc.*, 1987, **109**, 5541-5542.
- 3 P. J. Carson, C. R. Bowers and D. P. Weitekamp, *J. Am. Chem. Soc.*, 2001, **123**, 11821-11822.
- 4 M. B. Franzoni, L. Buljubasich, H. W. Spiess and K. Münnemann, *J. Am. Chem. Soc.*, 2012, **134**, 10393-10396.
- 5 G. Pileio, M. Carravetta and M. H. Levitt, *Proc. Natl. Acad. Sci. U. S. A.*, 2010, **107**, 17135-17139.
- 6 M. C. D. Tayler and M. H. Levitt, *Phys. Chem. Chem. Phys.*, 2011, **13**, 5556-5560.
- 7 Y. Feng, R. M. Davis and W. S. Warren, *Nat. Phys.*, 2012, **8**, 831-837.
- 8 T. Theis, Y. Feng, T. Wu and W. S. Warren, *J. Chem. Phys.*, 2014, **140**, 014201.
- 9 M. B. Franzoni, D. Graafen, L. Buljubasich, L. M. Schreiber, H. W. Spiess and K. Münnemann, *Phys. Chem. Chem. Phys.*, 2013, **15**, 17233-17239.

- 10 S. J. DeVience, R. L. Walsworth and M. S. Rosen, *Phys. Rev. Lett.*, 2013, **111**, 173002.
- 11 Y. Zhang, P. C. Soon, A. Jerschow and J. W. Canary, *Angew. Chem.*, 2014, **53**, 3396-3399.
- 12 W. S. Warren, E. Jenista, R. T. Branca and X. Chen, *Science*, 2009, **323**, 1711-1714.
- 13 Y. Feng, T. Theis, T. L. Wu, K. Claytor and W. S. Warren, *J. Chem. Phys.*, 2014, **141**, 134307.
- 14 G. Pileio, J. T. Hill-Cousins, S. Mitchell, I. Kuprov, L. J. Brown, R. C. D. Brown and M. H. Levitt, *J. Am. Chem. Soc.*, 2012, **134**, 17494-17497.
- 15 M. J. Frish, G. W. Trucks, *et al.*, Gaussian 09, Revision A.02, Gaussian, Inc., Wallingford CT, 2009.
- 16 A. Jerschow, *J. Magn. Reson.*, 2005, **176**, 714.
- 17 A. Jerschow, <http://www.nyu.edu/projects/jerschow/mathnmr.html>.
- 18 M. Carravetta and M. H. Levitt, *J. Chem. Phys.*, 2005, **122**, 214505.
- 19 M. H. Levitt, *Annu. Rev. Phys. Chem.*, 2012, **63**, 89-105.
- 20 G. Pileio, *Prog. Nucl. Mag. Res. Sp.*, 2010, **56**, 217-231.
- 21 G. Pileio, *J. Chem. Phys.*, 2011, **134**, 214505.
- 22 G. Pileio, *J. Chem. Phys.*, 2011, **135**, 174502.
- 23 G. Stevanato, S. S. Roy, J. Hill-Cousins, I. Kuprov, L. J. Brown, R. C. D. Brown, G. Pileio and M. H. Levitt, *Phys. Chem. Chem. Phys.*, 2015, **17**, 5913-5922.
- 24 M. C. D. Tayler and M. H. Levitt, *Phys. Chem. Chem. Phys.*, 2011, **13**, 9128-9130.
- 25 G. Pileio and M. H. Levitt, *J. Magn. Reson.*, 2007, **187**, 141-145.
- 26 A. Bornet, X. Ji, D. Mammoli, B. Vuichoud, J. Milani, G. Bodenhausen and S. Jannin, *Chem-Eur. J.*, 2014, **20**, 17113-17118.
- 27 D. Wolf and A. I. Kudish, *J. Phys. Chem.*, 1980, **84**, 921-925.
- 28 S. Z. M. a. W. R. Kimel, *J. Chem. Eng. Data*, 1961, **6**, 533-537.
- 29 G. Stevanato, J. T. Hill-Cousins, P. Hakansson, S. S. Roy, L. J. Brown, R. C. D. Brown, G. Pileio and M. H. Levitt, *Angew. Chem. Int. Ed. Engl.*, 2015, **54**, 3740-3743.

We show that a PHIP-originated singlet state in a chemically equivalent proton spin system can be revealed by a weak power spin-lock.

